JOURNAL OF Materials CHEMISTRY

Electronic and structural properties of the layered ternary carbide Ti_3AlC_2

Y. C. Zhou,* X. H. Wang, Z. M. Sun and S. Q. Chen

Ceramic and Composite Department, Institute of Metal Research, Chinese Academy of Sciences, 72 Wenhua Road, Shenyang 110016, P. R. China. Tel: +86-24-23843531 ext. 55180; Fax: +86-24-23891320; E-mail: yczhou@imr.ac.cn

Received 16th February 2001, Accepted 23rd May 2001
First published as an Advance Article on the web 30th July 2001

The electronic and structural properties of the layered ternary compound Ti_3AlC_2 have been determined using the *ab initio* pseudopotential method based on density functional theory. We have obtained the equilibrium lattice parameters, the equilibrium atomic positions in the unit cell, and interatomic distances. The calculated bulk modulus is 190 GPa and is comparable to that of TiC. The band structure, density of states (DOS) and effective charges are presented and compared with those of TiC. The band structure indicates that Ti_3AlC_2 is an electronic conductor. The electronic structure discloses that the bonding in Ti_3AlC_2 is anisotropic and metallic–covalent–ionic in nature. Compare to the structure of TiC, the presence of Al changes the Ti–C–Ti–C covalent bond chain into a Ti–C–Ti–C–Ti–Al bond chain through its reaction with Ti, forming the layered structure. Effective charge calculations suggest the ionic formula of Ti_3AlC_2 to be $(Ti^{1.18+})(Ti^{0.59+})_2(Al^{0.52-})(C^{0.92-})_2$.

1. Introduction

Recent discoveries of unconventional properties in the layered ternary carbides referred to as '312' phases have stimulated a growing demand for realistic theoretical studies of these systems. The common formula of these layered ternary compounds is T_3MC_2, where T is a transition metal, M is a group IIIA or IVA element, and C is carbon. These layered ternary carbides exhibit a unique combination of properties such as high strength and modulus, damage tolerance at room temperature, high electrical conductivity, low density, and being machinable with conventional high-speed tools without lubrication.[1–10] Titanium aluminium carbide (Ti_3AlC_2) is one of the interesting materials from this family. Interest in Ti_3AlC_2 emanates from the opportunity provided to tailor properties, since two distinct structurally related layered ternaries Ti_3AlC_2 and Ti_2AlC are available in the Ti–Al–C system. Furthermore, the density of Ti_3AlC_2 is lower than that of other '312' phases such as Ti_3SiC_2 and Ti_3GeC_2, which is attractive when it is used as a structural material or as a reinforcement for polymers and metals. The macroscopic properties of Ti_3AlC_2 are believed to be strongly related to the electronic and structural properties of the compound and we are interested to establish the relations between them.

Quantum mechanical modeling of solids through first-principles calculations has been proven to be a powerful tool for obtaining microscopic information, which is helpful in understanding the macroscopic properties of solids. Thus, investigation of the electronic structure and bonding properties is essential to understanding the various properties of Ti_3AlC_2. The electronic structure and bonding properties of Ti_3SiC_2 and Ti_3GeC_2 were investigated and published in previous work.[11–13] However, less information on the electronic structure and chemical bonding properties of Ti_3AlC_2 is available.[14] In this work, we investigate the atomic and electronic structure, and bonding properties of Ti_3AlC_2 using the *ab initio* total-energy pseudopotential method based on density functional theory (DTF).[15–17] While a complete understanding of the properties of Ti_3AlC_2 would require incorporating the effects of a high concentration of defects, calculations for the ideal structure should provide a useful starting point for further analysis.

2. Crystal structure and calculation details

Before examining the electronic structure of Ti_3AlC_2, it is relevant to consider the crystal structure of TiC since the structures of the two compounds are strongly related.[18] TiC crystallizes in the NaCl-type structure (space group *Fm*3*m*) with four formulae per unit cell. Ti and C atoms are at the origin and (1/2, 1/2, 1/2) positions, respectively. Ti and C are octahedrally coordinated with each other, consequently, Ti_6C octahedra share edges.

Ti_3AlC_2 has a crystal structure isotopic with that of Ti_3SiC_2 and a hexagonal symmetry with lattice parameters of $a=0.30753$ nm and $c=1.8578$ nm.[19] The space group is $P6_3/mmc$ and the atoms are located at the following (Wyckoff) positions: Ti at *2a* and *4f* ($Z_{Ti}=0.1280$), Al at *2b* and C at *4f* ($Z_C=0.5640$). The crystal structure of Ti_3AlC_2 is shown in Fig. 1. The structure can be described as two edge-shared Ti_6C octahedral layers separated by a two-dimensional closed-packed layer of Al. For the convenience of discussion, we define the Ti atoms located at *2a* positions as Ti(1) and those located at *4f* positions as Ti(2).

For the ground-state electronic structure calculations we have used the CASTEP code. CASTEP is a density functional theory-based pseudopotential total-energy code that employs special point integration over the Brillouin zone and a plane-wave basis set for the expansion of the wave functions. The CASTEP code has been well described in the literature.[17] One of the main traits of the CASTEP code is that the internal coordinates can be automatically relaxed so that the structure with the minimum total energy is obtained. The norm-conserving pseudopotentials for Ti, Al and C were generated using the optimized version of Kerker's scheme[20] and transformed into the separable form of Kleinman–Bylander pseudopotentials.[21] A gradient-corrected form of the exchange-correlation functional (generalized gradient approximation (GGA-PW91)) was used. The calculations have been

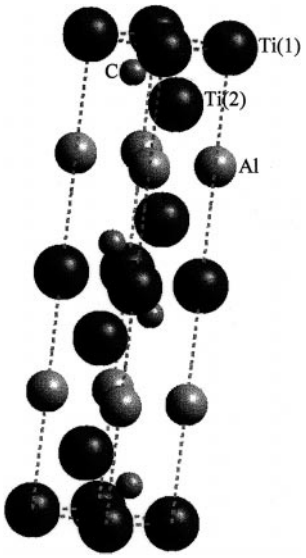

Fig. 1 Crystal structure of Ti_3AlC_2, the Ti atoms at *2a* positions are defined as Ti(1) and those at *4f* positions are defined as Ti(2).

performed using a plane-wave cutoff of 670 eV. This cutoff yields well-converged properties of the fully relaxed structure. Brillouin zone (BZ) sampling was performed using a Monkhorst–Pack special k-points mesh.[22]

3. Results and discussion

3.1 Optimization of structure

To calculate the ground-state electronic properties of Ti_3AlC_2, it is necessary to find the most stable atomic configuration of the crystal. The equilibrium structure has been determined by relaxation with respect to the lattice parameters and the internal parameter. For Ti_3AlC_2, only the Ti and C atoms at *4f* positions are movable. In Table 1, the calculated lattice constants and internal parameters for both Ti_3AlC_2 and TiC are listed and are compared with experimental data. The lattice parameters are in satisfactory agreement with the experimental values. The error in the lattice constant is 0.39% for TiC, and −0.11% for *a* and 0.83% for *c* of Ti_3AlC_2. The experimental fractional atomic coordinates for both Ti and C atoms in Ti_3AlC_2 are also well reproduced.

The total energy (TE) calculation is repeated for different volumes. At the equilibrium volume, we calculated the bulk moduli of Ti_3AlC_2 and TiC from the total energy–volume curves. The calculated TE data were fitted to the Murnaghan equations of states (EOS).[23] The estimated bulk moduli are 209 GPa for TiC and 190 GPa for Ti_3AlC_2, respectively. The reported bulk modulus of TiC measured in early work[24] was 220 GPa and our calculated bulk modulus is 5% lower than that value, which is quite consistent. Up to now, to the best of our knowledge, no study has been reported on the bulk modulus of Ti_3AlC_2. The bulk modulus of Ti_3SiC_2 deduced from the volume *vs.* pressure data by Onodera *et al.*[25] was 206 GPa, which is close to that of TiC. Ti_3AlC_2 is isostructural with Ti_3SiC_2 and shares many of its characteristics. Considering the reported Young's moduli[8] of Ti_3SiC_2 and Ti_3AlC_2 were 333 GPa and 297 GPa, respectively, the estimated bulk modulus of 190 GPa, which is a little smaller than that of Ti_3SiC_2, seems reasonable.

Table 1 Comparison of the calculated and experimental lattice parameters and fractional atomic coordinates for Ti_3AlC_2 and TiC

Lattice parameters			
Ti_3AlC_2		TiC	
$a_{exp.} = 3.0753$ Å[19]	$a_{calc.} = 3.0720$ Å	$a_{exp.} = 4.327$ Å	$a_{calc.} = 4.344$ Å
$c_{exp.} = 18.578$ Å[19]	$c_{calc.} = 18.732$ Å		

Fractional atomic coordinates of Ti_3AlC_2			
Ti(1)	Ti(2)	Al	C
0, 0, 0	1/3,2/3, *z*	0, 0, 1/4	1/3, 2/3, *z*
	$Z_{Ti\ exp.} = 0.1280$[19]		$Z_{C\ exp.} = 0.5640$[19]
	$Z_{Ti\ calc.} = 0.1290$		$Z_{C\ calc.} = 0.5701$

Table 2 Bond lengths (Å) of Ti_3AlC_2, TiC and Ti_2AlC

Compound	Ti–C	Ti(1)–C	Ti(2)–C	Ti–Al	Ti(1)–Ti(2)
Ti_3AlC_2		2.2068	2.0886	2.8783	2.9972
TiC	2.1722 (2.165)[26]				
Ti_2AlC	2.12[26]			2.85[26]	

We analyzed the bond lengths at equilibium atomic configuration, which are listed in Table 2. The calculated bond length of Ti–C in TiC (2.1722 Å) is close to the experimental value[26] (2.165 Å). It is interesting to note that the bond lengths of Ti(1)–C and Ti(2)–C are different in Ti_3AlC_2. The bond length of Ti(1)–C is longer than that of Ti–C in TiC while the bond length of Ti(2)–C in Ti_3AlC_2 is shorter than that of Ti–C in TiC. The same tendency was found in Ti_3SiC_2, *i.e.* the Ti–C bonds adjacent to the Si layers are shorter than those in the center of the unit cell.[27] From the above evidence and the fact that introducing a third element (Al) into the structure changes the bonding environment of Ti atoms, the difference of Ti–C bond lengths in Ti_3AlC_2 and TiC should not be surprising. Jeitschko *et al.*[26] compared the Ti–C bond lengths in perovskite Ti_3AlC (2.08 Å), H-phase Ti_2AlC (2.12 Å) and TiC (2.16 Å). Compared with these data, it is seen that the calculated bond length of Ti(2)–C in Ti_3AlC_2 is consistent with that in Ti_3AlC. The interatomic distance Ti–Al is 2.878 Å, which is slightly longer compared to the bond length of Ti(1,2)–C. If the difference in the atomic size between Al and C is ignored, the longer interatomic distance between Ti and Al indicates that the bonding between them is relatively weak. Since no experimental data for the bond lengths of Ti_3AlC_2 are available, the bond lengths calculated from the full relaxation of the internal coordinates are important for further discussion of the detailed structure of Ti_3AlC_2.

The effective charges, Q^* per atom in TiC and in Ti_3AlC_2 are calculated using the Mulliken scheme and are listed in Table 3. The values listed in Table 3 indicate a substantial covalent bonding character in both TiC and Ti_3AlC_2. On the basis of these calculated effective charges, we may write the ionic formulae for TiC and Ti_3AlC_2 as $(Ti^{+0.94})(C^{-0.94})$ and $(Ti^{+1.18})(Ti^{+0.59})_2(Al^{-0.52})(C^{-0.92})_2$, respectively.

3.2 Electronic structure of Ti_3AlC_2

At the equilibrium cell volume, we performed band-structure and density of state (DOS) calculations aimed at obtaining microscopic understanding of the electronic structure. Fig. 2(a) shows the energy bands of Ti_3AlC_2 along high-symmetry lines of the Brillouin zone while Fig. 2(b) shows the total density of states for Ti_3AlC_2. This exhibits normal metallic behavior with bands crossing the Fermi level along various directions, which results in a finite DOS (3.72 states/eV cell) at the Fermi level, as shown in Fig. 2(b). As a result, Ti_3AlC_2 will exhibit metallic properties such as metallic conductivity, which is analogous to Ti_3SiC_2 and Ti_3GeC_2.[11–13] The band structure also shows a strongly anisotropic feature with less *c*-axis energy dispersion. The anisotropy of the band structure near and below E_F

Table 3 Calculated effective charges for TiC and Ti_3AlC_2

Compound	Q_{Ti}^*	$Q_{Ti(1)}^*$	$Q_{Ti(2)}^*$	Q_{Al}^*	Q_C^*
Ti_3AlC_2		2.82	3.41	3.52	4.92
TiC	3.06				4.94

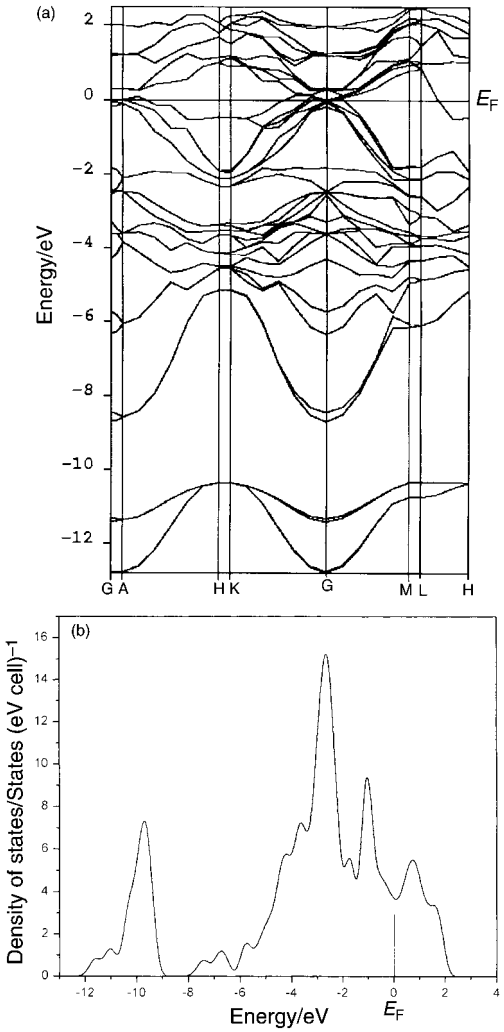

Fig. 2 Band-dispersion curve of Ti_3AlC_2 along the high-symmetry directions of the BZ (a), and the total density of states of Ti_3AlC_2 (b).

indicates that the conductivity is also anisotropic for single-crystal Ti_3AlC_2, *i.e.* the electrical conductivity along the *c* direction will be lower than that in the *ab* plane.

The bonding properties of Ti_3AlC_2 can be seen from the partial density of states of each element shown in Fig. 3. It is seen from Fig. 3 that the width of the Al 3s state is much larger than that of C 2s state and there are a number of peaks in the Al 3s state. The characteristics of the Al 3s state indicate that there are s–p interactions in Al, *i.e.* the close-packed layer of Al atoms are bonded through s–p interactions. For the energy range from −5 to −2 eV, there is a high degree of hybridization of Ti 3d with C 2p states, which is indicative of a covalent interaction. The pd hybridization or p–d bonding stabilizes the structure. Thus, in Ti_3AlC_2, Ti 3d–C 2p hybridization is the driving bonding force, which is analogous to the bonding properties in Ti_3SiC_2 and Ti_3GeC_2.[11–13] For the energy window from −2 to E_F, the Al 3p state interacts with the 3d state of Ti(2). At around the Fermi level, the DOS mainly originates from *nearly free-electron* states of Ti(2) 3d and Ti(1) 3d. Above the Fermi level, antibonding Ti(1,2) 3d states dominate with less contribution from Al 3p states. To further understand the electronic structure of Ti_3AlC_2, it is useful to compare the DOS and PDOS of Ti_3AlC_2 with those of TiC. Fig. 4 shows the total DOS (Fig. 4(a)) and the PDOS (Fig. 4(b)) of TiC that is broken up into site and angular momentum contributions. It is seen from the figure that in the valence band and from E_F to higher energies, Ti 3d and C 2p states have strongly similar shapes, which is indicative of a covalent interaction between them. Previous work by Mater *et al.*[28] demonstrated that in TiC, Ti

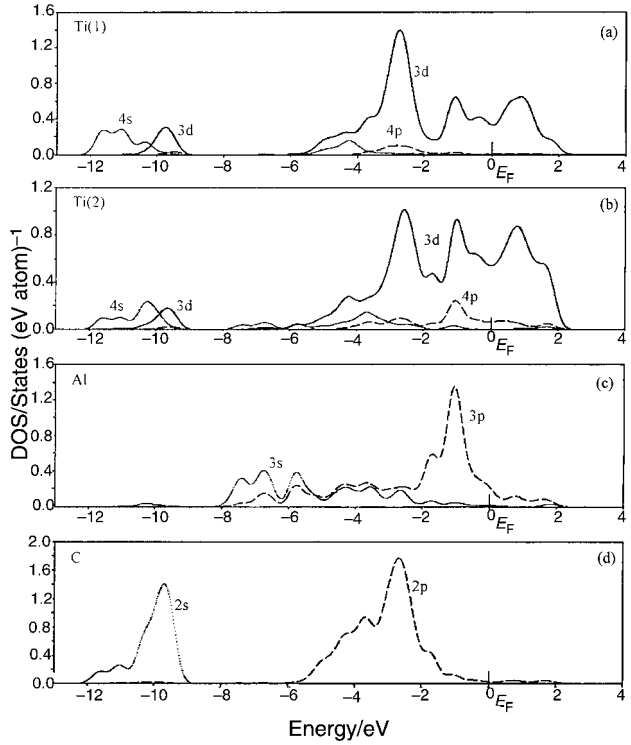

Fig. 3 Partial density of states of Ti(1) (a), Ti(2) (b), Al (c) and C (d) atoms (dotted lines indicate s states, long-dashed lines p states and solid lines d states).

3d–C 2p bonding is the driving force. The covalent Ti–C bond is directional leading to the Ti–C–Ti–C bond chain in the structure. Comparing the DOS and PDOS for Ti_3AlC_2 and TiC, it is seen that there is an increase in the amount of d character in the valence band of Ti_3AlC_2, *i.e.* introducing a third element (Al) leads to a recognizable increase in 3d character of the Ti atom in the valence band. The 3d state of the Ti(2) atom around the Fermi level also increases significantly due to the introduction of Al, *i.e.* Ti(2) 3d states dominate at around E_F and contribute to the metallic bonding.

3.3 Charge-density distribution

Fig. 5 shows the distribution of the valence charge density in the $(11\bar{2}0)$ plane of Ti_3AlC_2. For the convenience of discussion, a $2\times2\times1$ cell was used in Fig. 5. The figure reveals that titanium and carbon atoms form a Ti(2)–C–Ti(1)–C–Ti(2) covalently bonded chain, which is strongly directional. Each pair of Ti(2)–C–Ti(1)–C–Ti(2) bond chains share one Al atom, forming a Ti(2)–C–Ti(1)–C–Ti(2)–Al chain. In other words, the presence of Al changes the Ti(2)–C–Ti(1)–C–Ti(2) bond chain into a Ti(2)–C–Ti(1)–C–Ti(2)–Al bond chain, forming a layered structure. In the Ti(2)–C–Ti(1)–C–Ti(2) bond chain, the interatomic distance between Ti(1) and C is 2.2068 Å and that between Ti(2) and C is 2.0886 Å. This difference in bond lengths can easily be seen from the difference of charge density distribution between Ti(1)–C and Ti(2)–C in Fig. 5. The distance between Al and Ti(2) is 2.8783 Å, which indicates relatively weak bonding between Al and the Ti(2)–C–Ti(1)–C–Ti(2) covalent bond chain. The relatively weak bonding between Al and the Ti(2)–C–Ti(1)–C–Ti(2) bond chain allows easy slip between them and may correspond to the ultralow basal plane friction coefficient.[29] In Fig. 5, the distribution of charge density is spherical around carbon but not so around either titanium or aluminium atoms. The charge density is pulled from titanium atoms toward both carbon and aluminium atoms. This situation is caused mainly by the difference in the electronegativities; according to the Pauling scale, carbon and aluminium atoms are more

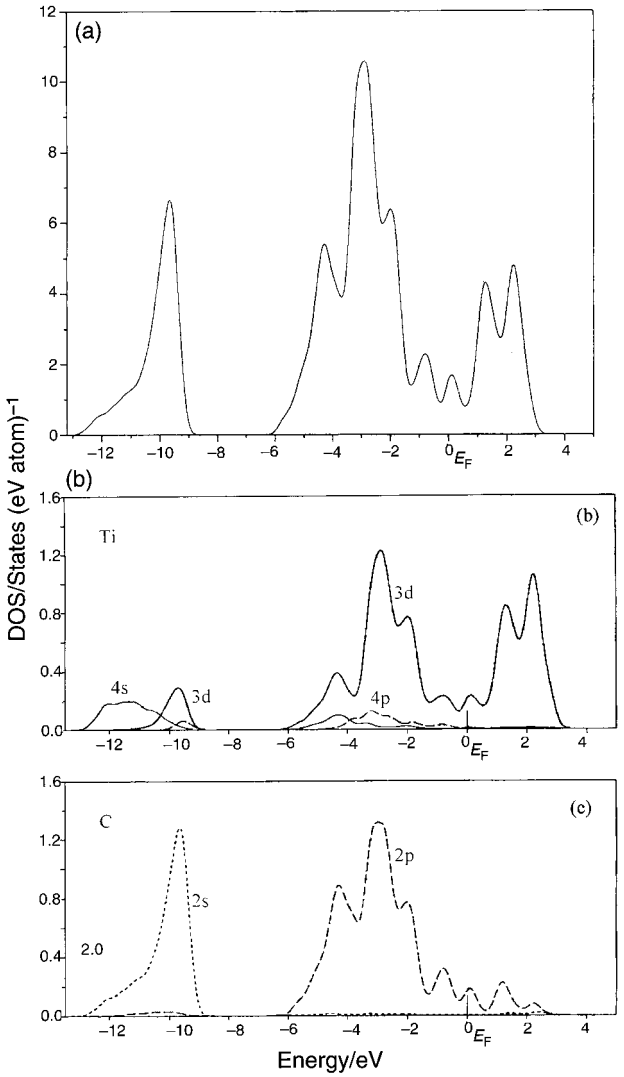

Fig. 4 Total DOS (a) and site-projected DOS of Ti and C in TiC (b, c) (dotted lines indicate s states, long-dashed lines p states and solid lines d states).

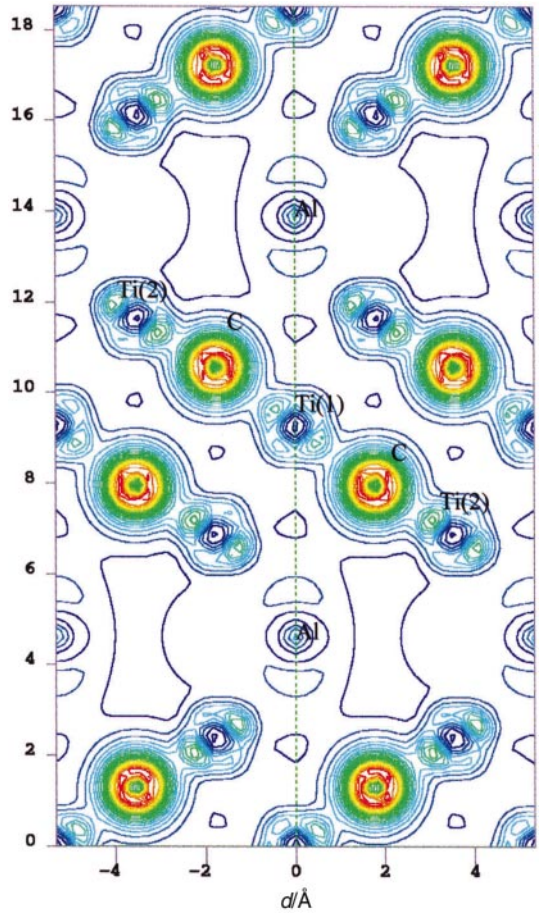

Fig. 5 Distribution of charge density on the $(11\bar{2}0)$ plane of Ti_3AlC_2; charge-density contours are from 0.05176 (dark blue) to 1.71539 au^{-3} (red) with a spacing of 0.08756 au^{-3}.

electronegative than titanium. From the analysis of the distribution of charge density shown in Fig. 5, the Ti–C bond can be described in terms of both ionic and covalent character and the Ti–Al bond can be described by mixed covalent, ionic and metallic character. The high strength and modulus are due to the strong Ti–C bonding, while the metallic electrical conductivity and easy basal plane slip are attributed to the metallic bonding between Ti(2) and Al in the structure.

4. Conclusions

We have used the *ab initio* total-energy pseudopotential method to investigate the electronic and structural properties of the layered ternary carbide Ti_3AlC_2. The equilibrium lattice parameters of $a=3.0720$ Å and $c=18.732$ Å and atomic positions have been obtained. The band structure, density of states and effective charges have been presented and are compared with those of TiC. The band structure indicates that Ti_3AlC_2 is an electronic conductor, and that the bonding in Ti_3AlC_2 is anisotropic and metallic–covalent–ionic in nature. Compared to the electronic structure of TiC, the presence of Al in Ti_3AlC_2 leads to the increase of d character in the valence band and around the Fermi level. The interatomic distances at equilibrium configuration between Ti–C are 2.0886 Å and 2.2068 Å, respectively, demonstrating strong covalent bonding between Ti and C. The bonding between Ti and Al is, however, relatively weak and the weak bonding may correspond to the easy slipping observed in the structure. Based on the calculated effective charges, the ionic formula of Ti_3AlC_2 could be given by $(Ti^{1.18+})(Ti^{0.59+})_2(Al^{0.52-})(C^{0.92-})_2$.

Acknowledgements

This work was supported by National Outstanding Young Scientist Foundation of China for Y. Zhou under Grant No.59925208, National Science Foundation of China under Grant No. 50072034 and the 863 Program.

References

1 Y. C. Zhou, Z. M. Sun, S. Q. Chen and Y. Zhang, *Mater. Res. Innovations*, 1998, **2**, 142.
2 I. M. Low, *J. Eur. Ceram. Soc.*, 1998, **18**, 709.
3 Y. C. Zhou and Z. M. Sun, *Mater. Res. Innovations*, 1999, **2**, 360.
4 Y. C. Zhou and Z. M. Sun, *Mater. Res. Innovations*, 1999, **3**, 171.
5 Z. M. Sun, Y. C. Zhou and J. Zhou, *Philos. Mag. Lett.*, 2000, **80**, 289.
6 S. Arunajatesan and A. H. Carim, *Mater. Lett.*, 1994, **20**, 319.
7 Y. C. Zhou, Z. M. Sun, J. H. Sun, Y. Zhang and J. Zhou, *Z. Metallkd.*, 2000, **91**, 329.
8 N. V. Tzenov and M. W. Barsoum, *J. Am. Ceram. Soc.*, 2000, **83**, 825.
9 Y. C. Zhou, Z. M. Sun and B. H. Yu, *Z. Metallkd.*, 2000, **91**, 937.
10 I. M. Low, S. K. Lee and B. R. Lawn, *J. Am. Ceram. Soc.*, 1998, **81**, 225.
11 Z. M. Sun and Y. C. Zhou, *Phys. Rev. B*, 1999, **60**, 1441.
12 Y. C. Zhou and Z. M. Sun, *J. Phys.: Condens. Mater.*, 2000, **12**, L457.
13 Y. C. Zhou and Z. M. Sun, *J. Mater. Chem.*, 2000, **10**, 343.
14 A. L. Ivanovski and N. I. Medvedeva, *Mendeleev Commun.*, 1999, **1**, 36.

15 P. Hohenberge and W. Kohn, *Phys. Rev. B*, 1964, **136**, 864.
16 W. Kohn and L. J. Sham, *Phys. Rev. A*, 1965, **140**, 1133.
17 M. C. Payne, M. P. Teter, D. C. Allan, T. A. Arias and J. D. Joannopoulos, *Rev. Mod. Phys.*, 1992, **64**, 1045.
18 Y. C. Zhou and Z. M. Sun, *Mater. Res. Innovations*, 2000, **3**, 286.
19 M. A. Pietzka and J. C. Schuster, *J. Phase Equilib.*, 1994, **15**, 392.
20 J.-S. Lin, A. Qteish, M. C. Payne and V. Heine, *Phys. Rev. B*, 1993, **47**, 4174.
21 L. Kleinman and D. M. Bylander, *Phys. Rev. Lett.*, 1982, **48**, 1425.
22 H. J. Monkhorst and J. D. Park, *Phys. Rev. B*, 1976, **13**, 5188.
23 F. D. Murnagahn, *Proc. Natl. Acad. Sci. USA*, 1944, **30**, 244.
24 H. G. Drickamer, R. W. Lynch, R. L. Clendenen and E. A. Perez-Alubuerne, in *Solid State Physics*, ed. F. Seitz and D. Turnbull, Academic Press, New York, 1996, vol. 19, p. 135.
25 A. Onodera, H. Hirano, T. Yuasa, N. F. Gao and Y. Miyamoto, *Appl. Phys. Lett.*, 1999, **74**, 3782.
26 W. Jeitschko, H. Nowotny and F. Benesovsky, *J. Less-common Met.*, 1964, **7**, 133.
27 M. W. Barsoum, T. El-Raghy, C. J. Rawn, W. D. Porter, A. Payzant and C. R. Hubbard, *J. Phys. Chem. Solids*, 1999, **60**, 429.
28 S. F. Mater, Y. L. Petitcorps and J. Etourneau, *J. Mater. Chem.*, 1997, **7**, 99.
29 A. Crossley, E. Kisi, J. W. B. Summers and S. Myhra, *J. Phys. D: Appl. Phys.*, 1999, **32**, 632.